Yielding Characteristics of Sand under Triaxial Compression and Extension Stresses

By Norihiko MIURA*, Noriyuki YASUFUKU**
and Takashi YAMAMOTO***

(Received July 14, 1982)

Abstract

Yield curves of sand in a particle-crushing region were determined by the multi-step stress path method with a high pressure triaxial apparatus. The yield curves depicted on the $p-q$ diagram were found to have such characteristics as $dq/dp=G(\eta)$, irrespective of stress path, where q is deviator stress, p is mean principal stress, and η is stress ratio. Integrating the $dq/dp \sim \eta$ curve numerically, the $\eta - U_p(\eta)$ relationship was obtained, by which a family of yield curves was constructed. It was shown that the yield curves of a family are similar with respect to the origin of the $p-q$ diagram and hence they can be normalized so as to form a single curve by using a newly defined stress parameter p_e.

Introduction

The mechanical behaviors of granular soil in particle-crushing regions were investigated by triaxial compression tests over a wide range of confining pressures from 100 kPa to 50 MPa, and the following experimental results have been obtained[2)~4)].

The compressibility of granular soil considerably increases due to particle-crushing, hence the slope of $e-ln\ p$ curve becomes as large as comparable to that of normally consolidated clay. At the stress that particle-crushing initiates, the $e-ln\ p$ curve forms a corner. This stress may be regarded as a kind of yielding stress. A stress range higher than the yielding stress is referred to as the called paricle-crushing region[4)].

The effect of particle-crushing on the shear strength may be explained as follows: the particle-crushing causes decrease in dilatancy effect, resulted in a decrease in the shear strength of the material. That is, the greater the dilatancy effect of a specimen, the more the decrease of shear strength due to particle-crushing results.

Stress strain characteristics are also affected by particle-crushing: axial strain at failure shifts to a larger value and the volumetric strain increases towards contraction, and the peak of the stress strain curve loses its sharpness. This penomenon may be interpreted that a strain softening material becomes a strain hardening material owing to particle-crushing.

Taking into consideration the change in the stress strain characteristics stated above, the authors found as indicated in the previous paper[4)] that the stress strain

* Department of Construction Engineering
** Graduate Student, Construction Engineering
*** Aoki Kensetsu Co., Ltd.

behavior of sand in a particle-crushing region can be roughly estimated using the Roscoe model[5] proposed for predicting the stress strain relationship of normally consolidated clay. There are some problems, however, in applying the Roscoe model to predict stress strain behavior of sand in a particle-crushing region. The most important and basic problem is the considerable difference of the observed and estimated yield curves.

To investigate this problem, the authors carried out multi-step stress path tests under the triaxial compression stresses with a high pressure triaxial apparatus on the Toyoura sand[4]. In this paper, multi-step stress path tests were made not only under the triaxial compression stresses but also under the extension stresses, and the general characteristics of the yield curve of sand in a particle-crushing region are discussed.

2. Specimen Preparation

The sample used in this study was the Toyoura sand B, which is different from the Toyoura sand used in the previous study[4] (sand A); however, the properties of these two sands are almost the same. The main properties of the Toyoura sand B are as follows; specific gravity = 2.64, maximum diameter = 0.25 mm, uniformity coefficient = 1.5, maximum void ratio = 0.92, and minimum void ratio = 0.58.

A fully saturated specimen in a loose state (initial void ratio was about 0.84) was molded to about 50 mm in diameter and 130 mm in height. The general procedure for the high-pressure triaxial compression test was essentially the same as that of the standard triaxial test at an ordinary confining pressure. As for the triaxial extension test, certain procedures were necessary for assembling the triaxial chamber as followings. As illustrated in Fig. 1, the upper pedestal ① was jointed to piston ② by a screw ③, following the completion of the triaxial chamber assembly. To avoid any twisting of

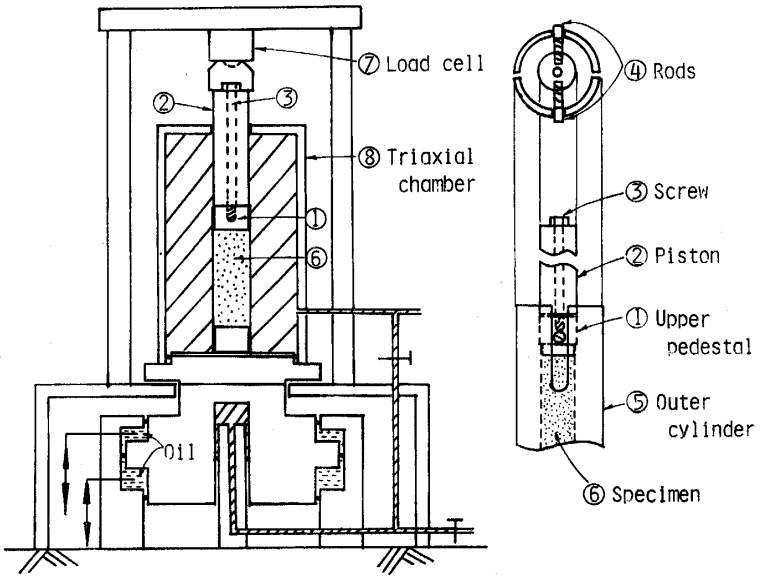

Fig. 1 Schematic diagram of high pressure triaxial apparatus.

specimen at the time of screw inserting, the rods ④ projecting from the upper pedestal are placed in the slits of the outer cylinder ⑤.

All specimen were consolidated isotropically by controlling the axial load P so that $\sigma_a=\sigma_r$, where σ_a is the axial stress and σ_r is the radial stress. Two types of extension tests were performed: the σ_a=constant type and the σ_r=constant type.

3. Material Constants

Three kinds of material constants, λ, κ and M, defined by Roscoe[5] were used in this study. The constant λ is the slope of $e-ln\,p$ curve in a normally consolidation (particle-crushing) region, i.e. $\lambda=(e_1-e_2)/ln(p_2/p_1)$, and the constant κ is the slope of the swelling curve of the $e-ln\,p$ relationship, as shown in Fig. 2. From this figure,

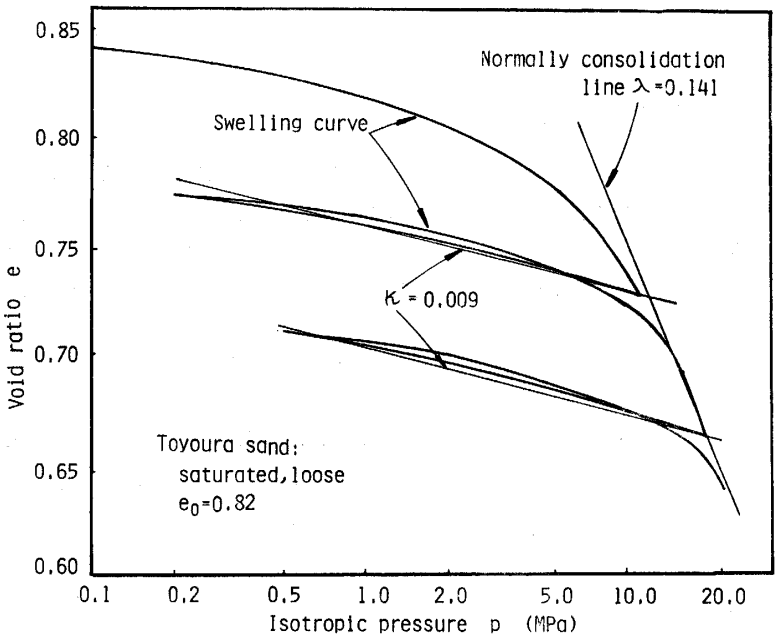

Fig. 2 Determination of soil constants λ and κ.

the magnitude of λ and κ of the sand B can be determined as $\lambda=0.141$ and $\kappa=0.009$ respectively, while in the case of the sand A, $\lambda=0.162$ and $\kappa=0.018$[3]. The constant M is a quantity concerned with the frictional property of the material, and is equal to the stress ratio $\eta=q/p$ at the critical state (=c.s.)[6]. Let σ'_a and σ'_r be the axial and radial effective principal stresses, then,

$$\begin{aligned} M&=(q/p)_{cs}=\eta_{cs}\\ q&=\sigma'_a-\sigma'_r \qquad (2)\\ p&=(\sigma'_a+2\sigma'_r)/3 \end{aligned}$$

The $p-q$ plots of the compression and extension test results are shown in Fig. 3, from

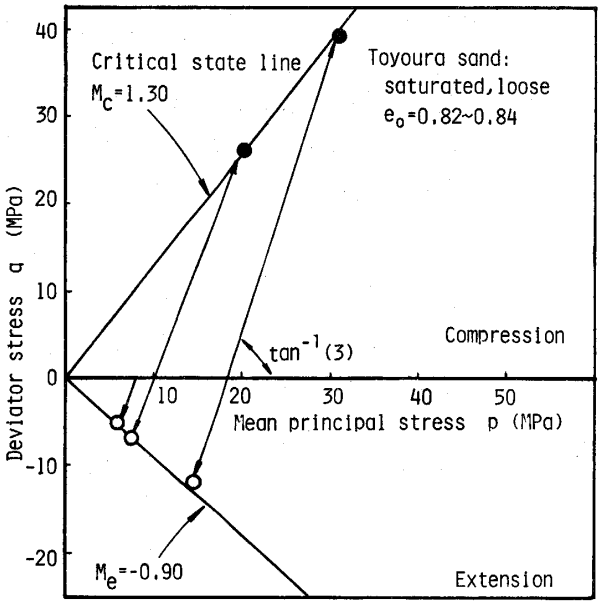

Fig. 3 p–q plot to determine the frictional constant M.

which we obtain $M_c=1.3$ and $M_e=-0.9$. The value of M_c of the sand A was also 1.30[4]. On the basis of the Mohr-Coulomb hypothesis that the internal friction angle under compression stresses ϕ'_c is the same as that under extension stresses ϕ'_e, the relationship between M_c and M_e can be expressed by the following equation,

$$M_e=\frac{-3M_c}{3+M_c} \tag{3}$$

Accepting the value of $M_c=1.30$, Eq. (3) predicts that $M_e=-0.907$ which is close to the observed value of -0.90. The stress parameters p and q are associated with the strain parameters v and ε, respectively. Let ε_a and ε_r be the axial and radial principal strains, then

$$\varepsilon=\frac{2}{3}(\varepsilon_a-\varepsilon_r) \tag{4}$$

$$v=\varepsilon_a+2\varepsilon_r$$

4. Multi-Step Stress Path Test

(1) Test program

A useful method for investigating the characteristics of a yield curve is to perform the multi-step stress path test using triaxial apparatus[4]. In this study, several kinds of multi-step stress path tests were performed under both compression and extension stress conditions, as shown in Fig. 4. Before the shearing, each specimen was isotropically consolidated at a given stress for about 16 hours. As for the isotropic consolidation of an extension specimen, the axial load P was maintained at $P=A\sigma_r$ during

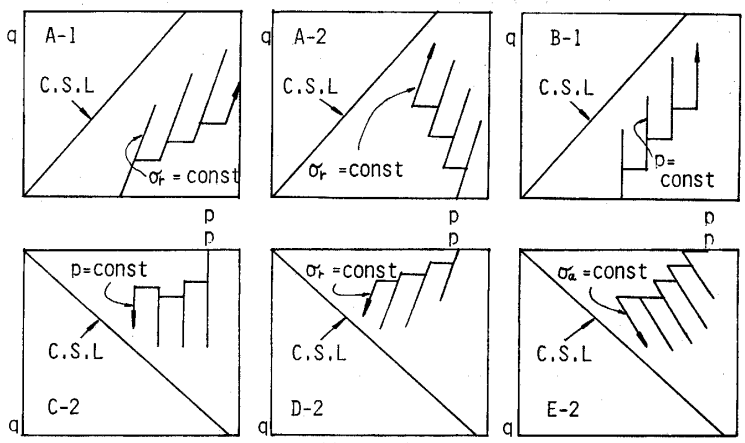

Fig. 4 Stress path for thr multi-step stree path test.

the consolidation, where A is cross-sectional area of the specimen. The specimen was then subjected to loading and unloading according to a given program. One cycle of loading and unloading required about two hours. The loading was carried out in 4 to 5 steps by the stress controlling method shown in Table 1. When the strain rate at a certain loading step became less than 0.01%/min (axial deformation 0.015 mm during 1 minute), the load was increased by a certain increment.

Table 1. Program of loading and unloading steps.

	σ_r (MPa)	p (MPa)	q (MPa)	η	$F(\sigma_r)$ (kN)	Load (kN)	DG (cm)	B (cm^3)
0	15	15.0	0	0	−0.23		3.50	13.30
0–1	15	14.7	−1.0	−0.07	−0.23	27.58	3.493	13.30
0–2	15	14.3	−2.0	−0.14	−0.23	25.77	3.486	13.30
0–3	15	14.0	−3.0	−0.21	−0.23	23.96	3.475	13.35
0–4	15	13.7	−4.0	−0.29	−0.23	22.16	3.461	13.50
1	15	13.3	−5.0	−0.38	−0.23	20.36	3.438	14.10
1–1	15	13.8	−3.5	−0.25	−0.23	23.56	3.452	14.30
2	15	14.3	−2.0	−0.14	−0.23	26.26	3.467	14.55
3	14	13.3	−2.0	−0.15	−0.23	23.82	3.464	14.40
3–1	14	13.0	−3.0	−0.23	−0.23	22.02	3.453	14.30
⋮	⋮	⋮	⋮	⋮	⋮	⋮	⋮	⋮

$F(\sigma_r)$=Piston friction, DG=Dial gage, B=Buret

(2) Determination of yield point

The stress strain curve of soil is generally of the shape of hyperbola[1]. Hence, the yield point on the stress strain curve is difficult to determine exactly. In the preceeding paper[4], several methods for determining the yield point were studied and it was concluded that the maximum curvature point on $q-\varepsilon$ or $p-v$ curve should be used as the yield point. This method was also used in the present study to determine the yield point.

(3) Formation of yield curve

From the yield point on either the $q-\varepsilon$ curve or $p-v$ curve, yield stresses q_y and p_y were determined, and are plotted on the stress paths drawn in the $p-q$ diagram shown in Fig. 5. In this figure, points 1 and Y are associated yield points, and the curve $\overset{\frown}{1\ Y}$ is a segment of the yield curve. In a similar manner, the curve $\overset{\frown}{4\ Y'}$ is a segment of another yield curve. As suggested in Fig. 5, the size of the yield curve including $\overset{\frown}{4\ Y'}$ is larger than that of the yield curve including $\overset{\frown}{1\ Y}$. Thus, when the larger yield curve is formed, the inner yield curve inevitably disappeas into the elastic region within the larger yield curve.

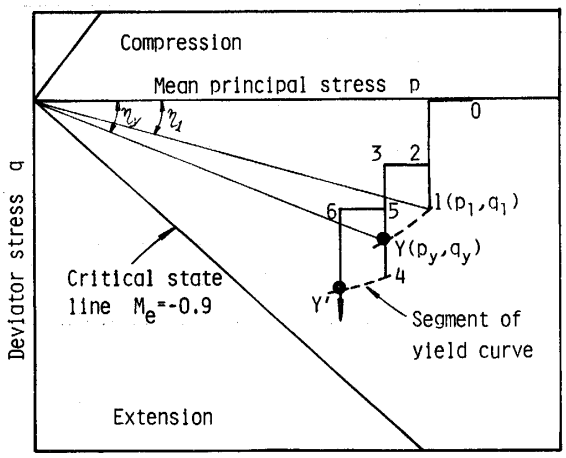

Fig. 5 Determination of segments of yield curves.

5. Characteristics of Yield Curve

(1) Experimental results

A typical stress strain curve obtained from the multi-step stress path test is shown in Fig. 6. The numbers indicate the loading steps described in Table 1. The various segments of the yield curve are depicted on the $p-q$ diagram as shown in Fig. 7. These curves were determined on the $q-\varepsilon$ curves. It is noted that the location of the two kinds of yield curves, determined on $q-\varepsilon$ curve and $p-v$ curve, are nearly the same, suggesting that the plastic distortional and volumetric strain occur simultaneously at a certain stress level[4]. Hence, we determined the yield curve based on the $q-\varepsilon$ curve in this study.

(2) Characteristics of yield curve

In regard to the characteristics of the yield curve under triaxial compression stress, the authors found that the slope of the yield curve in $p-q$ diagram, dq/dp, is uniquely related to the stress ratio[4], i.e.,

$$\frac{dq}{dp}=G(\eta) \tag{5}$$

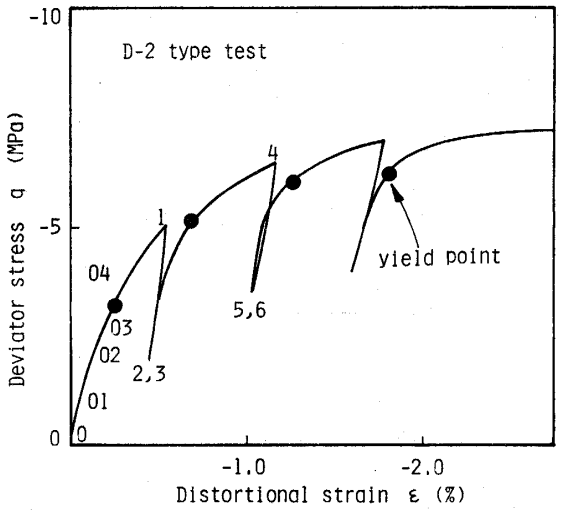

Fig. 6 Triaxial stress strain curve in the multi-step stress path test.

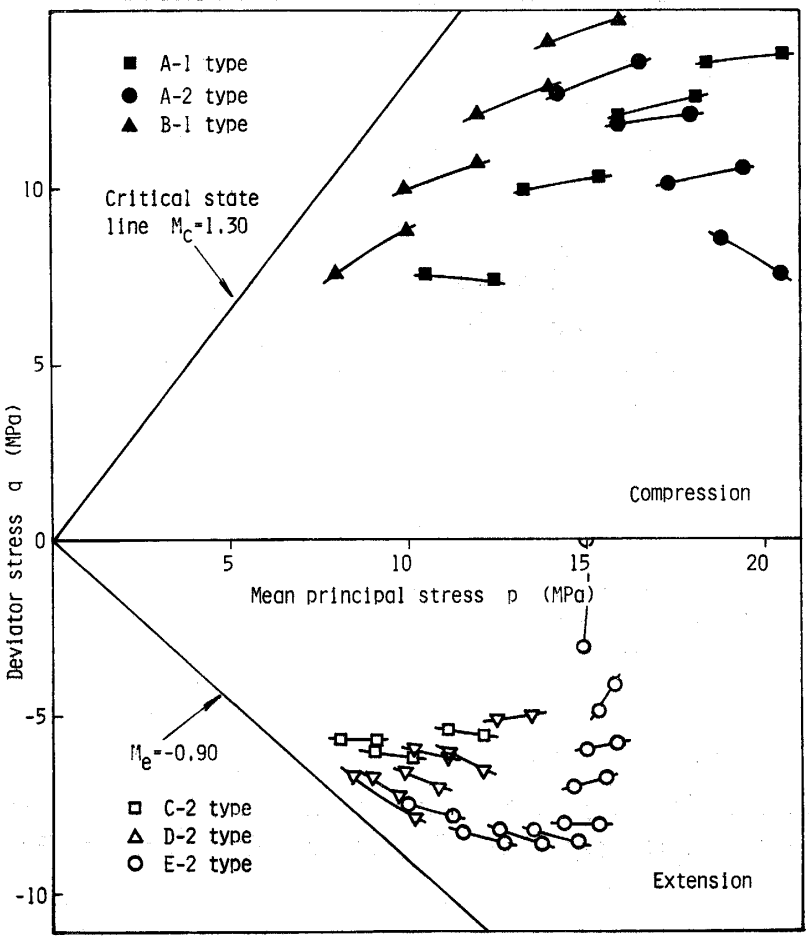

Fig. 7 Family of yield curve segments obtained under the triaxial compression and extension tests.

The same characteristics is expected to find under triaxial extension stress.

Referring to Fig. 5, let the stress parameters at points 1 and Y be (p_1, q_1, η_1) and (p_y, q_y, η_y), respectively. The values of dq/dp and η may thus be approximately evaluated by the following equations,

$$\frac{dq}{dp}=(q_1-q_y)/(p_1-q_y) \tag{6}$$

$$\eta=\frac{\eta_1+\eta_y}{2} \tag{7}$$

Figure 8 shows the $dq/dp-\eta$ characteristics of the yield curve segments presented in Fig. 7, which suggests Eq. (5) is also useful under the condition of extension stress. The experimental results above stated indicate that the characteristics of a yield curve of sand in a particle-crushing region depend on the stress ratio, irrespective of the stress path.

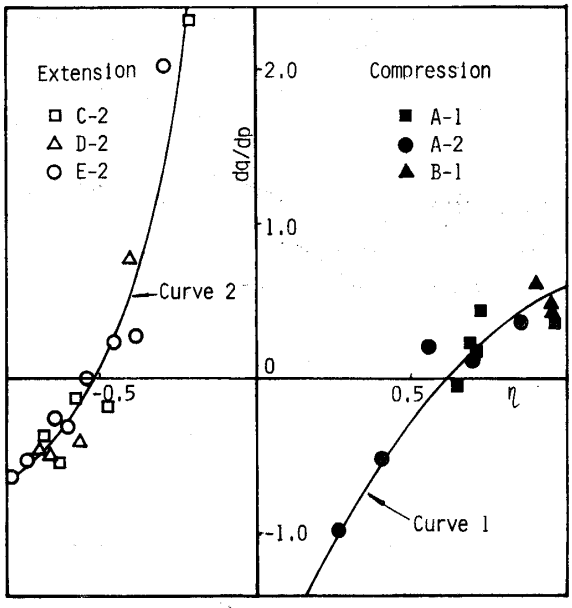

Fig. 8 dq/dp$-\eta$ characteristics of the yield curve segments represented in Fig. 7.

(3) Formation of yield curve

On the basis of Eq. (5), yield curve may be depicted as follows. From the equation $q=\eta p$, we obtain $dq=\eta dp+pd\eta$. Putting this relationship into Eq. (5) and integrating,

$$p=\frac{p_i}{U_P(\eta_i)}\cdot U_P(\eta)$$

$$q=\eta p \tag{8}$$

$$U_P(\eta)=\exp\left(\int_0^{\eta}\frac{1}{G(\eta)-\eta}\,d\eta\right)$$

where p_i is an integrating constant having the value of p corresponding to $\eta=\eta_i$ on the current yield curve. Now consider a new parameter p_e defined as the value of p corresponding to $\eta=0$. The parameter p_e is obtained from the first equation in Eq. (8), $p_{\eta=0}=p_e=(p_i/U_p(\eta_i))\cdot U_p(0)$, where $U_p(0)=1$. Hence,

$$p_e=\frac{p_i}{U_P(\eta_i)} \tag{9}$$

Therefore, Eq. (8) may also be expressed as,

$$\begin{aligned} p&=p_e\cdot U_p(\eta)\\ q&=\eta p \end{aligned} \tag{10}$$

To depict the yield curve on $p-q$ diagram based on Eq. (8) or (10), an arbitrarily chosen stress (p_i, η_i) is necessary along with the $\eta-U_p(\eta)$ relationship. So far, we have been unable to find the analytical relationship between $\eta-U_p(\eta)$, but it can be obtained by numerically integrating the $dq/dp-\eta$ curve, as shown in Fig. 9. Thus, we could depict the yield curves as shown in Fig. 10. The segments of the yield curves appearing in Fig. 7 are also shown. Comparing these two families of yield curves, it is evident that the yield curve based on Eq. (10) is well comparable with those observed.

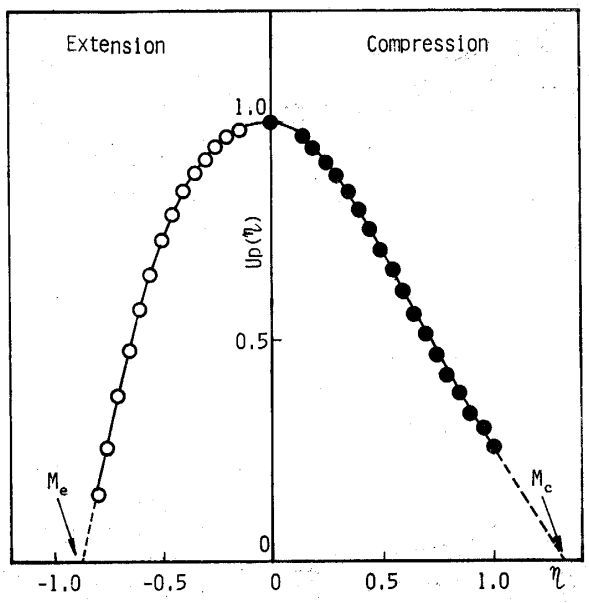

Fig. 9 $\eta-U_P(\eta)$ curve obtained by integrating the $dq/dp-\eta$ curve.

6. Normalization of Yield Curve

As stated previously, the yield curve of sand in a particle-crushing region is a function of the stress ratio, that is, yield curves of any size are similar with respect to

the origin of the $p-q$ diagram. This means that a family of the yield curves may be normalized and folded so as to become a single curve provided the stress parameter, such as p_e expressed by Eq. (9) is used. Graphical illustration of the parameter p_e is shown in Fig. 11, and formulated as,

$$p_e = \exp\left(\frac{e_n - e_s + \lambda \ln p_n - \kappa \ln p_s}{\lambda - \kappa}\right) \tag{11}$$

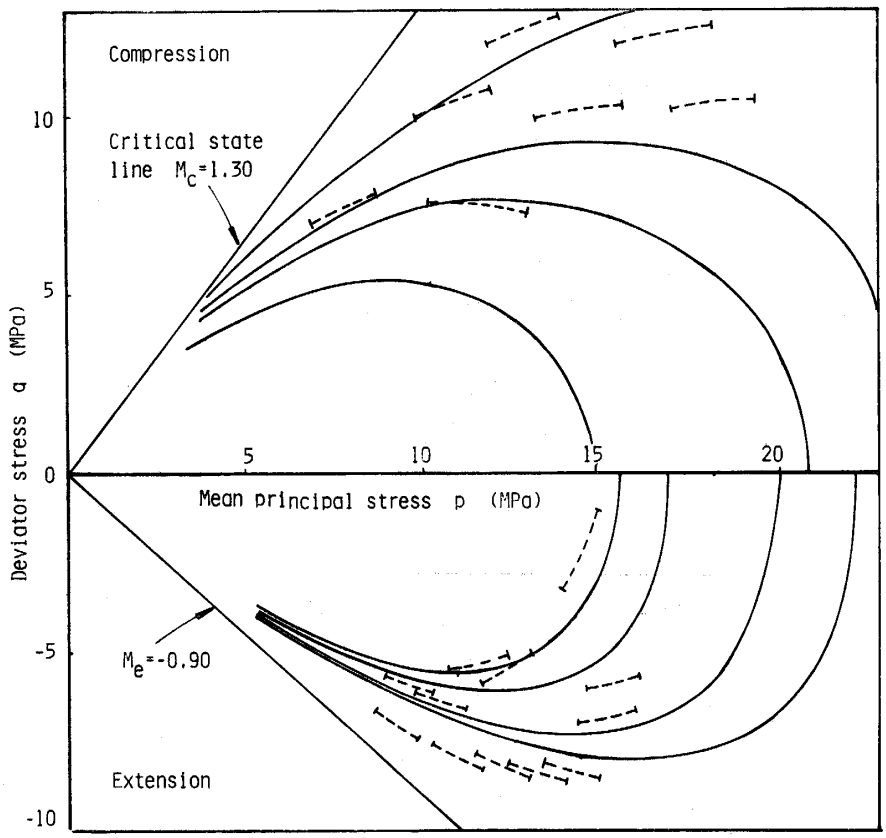

Fig. 10 Families of yield curves depicted from Fig. 9 and Eq. 10.

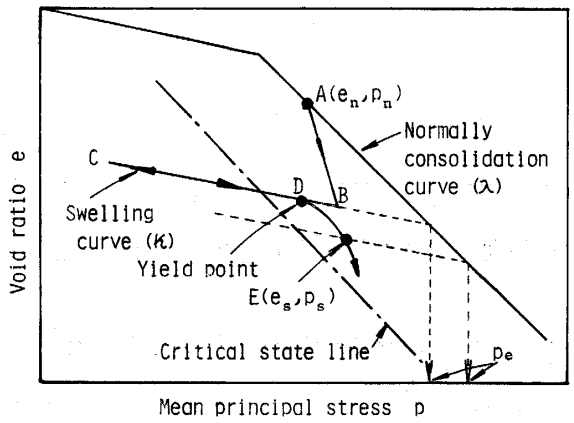

Fig. 11 Illustration of stress parameter p_e.

Using this stress parameter, Eq. (8) becomes,

$$p^* = p/p_e$$
$$q^* = q/p_e \tag{12}$$

The mapping of the yield curve on the p^*-q^* diagram is illustrated in Fig. 12. As suggested by this figure, triaxial test results of any stress paths are mapped on the p^*-q^* diagram and a unique normalized yield curve may be obtained. To confirm this, drained triaxial tests were performed both under compression and extension stresses at constant confining pressures. Test results are shown in Fig. 13, which indicate the relationship between e, p and p_e during the consolidation and shearing of the triaxial extension test. This result is plotted on the p^*-q^* diagram as shown in Fig. 14, together with the normalized yield curve determined from a constant volume test. In this figure, the yield curve shown in Fig. 10 is also shown for comparison with the experimental curves. It can be seen from this figure that the three kinds of curves are nearly the same, and that the whole yield curve over the compression and extension regions takes a shape of balloon.

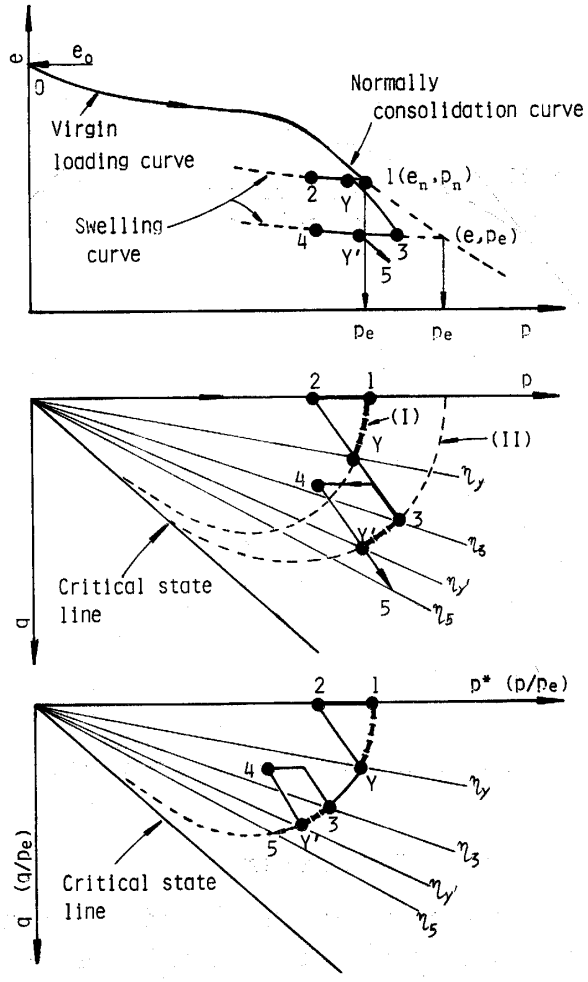

Fig. 12 Mapping of the yield curve on the p^*–q^* diagram.

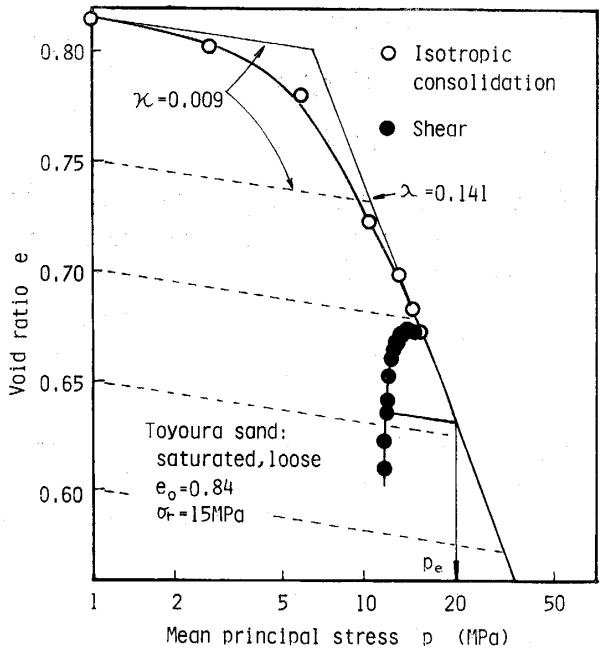

Fig. 13 e—log p curve of a drained triaxial compression test.

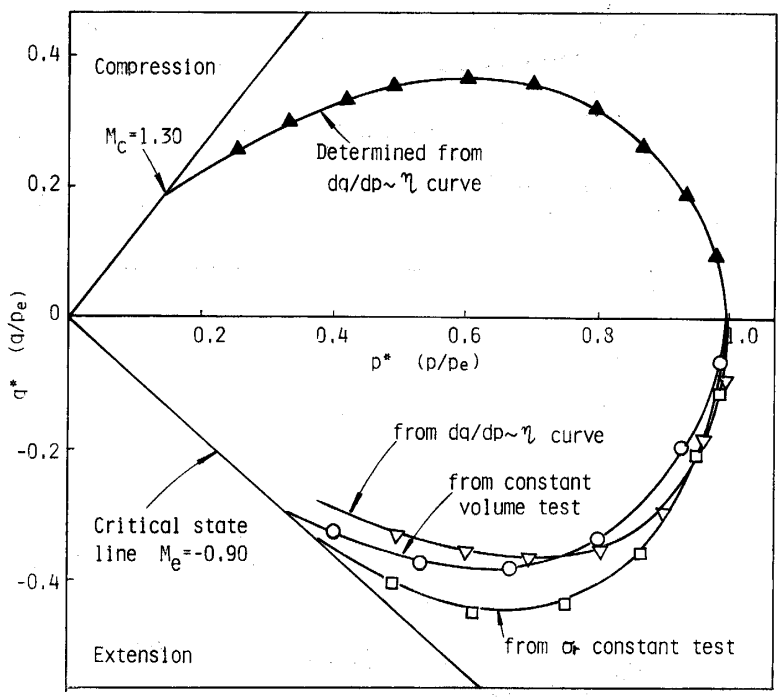

Fig. 14 Normalized yield curve determined from several method.

7. Conclusions

To investigate yield curve characteristics of sand in a particle-crushing region, multi-step stress path tests were carried out using high pressure triaxial apparatus on the Toyoura sand in saturated and loose states. The main conclusions obtained are

as follows.

(1) The values for the frictional constants M_c and M_e measured under compression and extension stresses are $M_c=1.30$ and $M_e=-0.90$. These values approximately satisfy the relationship $M_e=-3M_c/(3+M_c)$, derived from the Mohr-Coulomb hypothesis $\phi_{ext}=\phi_{comp}$.

(2) The characteristics of yield curves under triaxial extension stress may be expressed as $dq/dp=G(\eta)$ irrespective of stress path, as in the case of yield curves obtained under triaxial compression stress.

(3) Integrating the $dq/dp-\eta$ curve numerically, the $\eta-U_p(\eta)$ relationship is obtained, by which a family of yield curves can be formed. These yield curves were found to be quite well comparable with the yield curve segments obtained from triaxial compression and extension tests.

(4) The yield curves are similar in the form with respect to the origin of the $p-q$ diagram. Thus, the yield curves can be normalized and folded so as to form a single curve by using the stress parameter, p_e.

References

1) Kondner, R. L. and Zelasko, J. S., "Void ratio effects on the hyperbolic stress-strain response of a sand", Laboratory Shear Testing of Soils, ASTM, STP No. 361, pp. 250–257 (1963)
2) Miura, N. and Yamanouchi, T., "The effect of the particle-crushing on the shear characteristics of a sand", Proc. JSCE, No. 260, pp. 109–118 (1977)
3) Miura, N., "A consideration on the stress strain relationship of a sand under high pressures", Proc. JSCE, No. 282, pp. 127–130 (1979)
4) Miura, N. and Yamamoto, N., "On the yield curve of sand in particle-crushing regions", Proc. JSCE, No. 326, pp. 83–93 (1982)
5) Roscoe, K. H. and Burland, J. B., "On the generalized stress strain behaviour of "wet" clay", Engineering Plasticity, Cambridge Univ. Press., pp. 535–609 (1968)
6) Schofield, A. and Wroth, P., Critical State Soil Mechanics, McGraw-Hill Book Company, New York (1968)